The Major Histocompatibility Complex–related Fc Receptor for IgG (FcRn) Binds Albumin and Prolongs Its Lifespan

Chaity Chaudhury,[1] Samina Mehnaz,[1] John M. Robinson,[2] William L. Hayton,[3] Dennis K. Pearl,[4] Derry C. Roopenian,[5] and Clark L. Anderson[1]

[1]Department of Internal Medicine, [2]Department of Physiology and Cell Biology, [3]Department of Pharmacy, and [4]Department of Statistics, The Ohio State University, Columbus, OH 43210
[5]The Jackson Laboratory, Bar Harbor, ME 04609

Abstract

The inverse relationship between serum albumin concentration and its half-life suggested to early workers that albumin would be protected from a catabolic fate by a receptor-mediated mechanism much like that proposed for IgG. We show here that albumin binds FcRn in a pH dependent fashion, that the lifespan of albumin is shortened in FcRn-deficient mice, and that the plasma albumin concentration of FcRn-deficient mice is less than half that of wild-type mice. These results affirm the hypothesis that the major histocompatibility complex–related Fc receptor protects albumin from degradation just as it does IgG, prolonging the half-lives of both.

Key words: antibody • transport • half-life • pharmacokinetics • metabolism

Introduction

Albumin is a heart-shaped molecule of 67 kD that constitutes two-thirds of the protein mass of serum. Likened to a tramp steamer, it transports a great assortment of molecules such as fatty acids, bile acids, eicosanoids, vitamins, hormones, ions, toxins, and drugs. As well albumin endows blood with most of its colloid osmotic pressure and is the major pH buffering protein of serum (1).

For nearly a half century it has been known that the fractional catabolic rate of albumin is directly related to its serum concentration (2). Thus, the half-life of infused albumin in analbuminemic patients is as long as 115 d compared with 20 d in the normal individual (3). This same direct relationship of concentration to catabolism is characteristic of IgG, but not of several other serum proteins such as fibrinogen, transferrin, haptoglobin, IgA, and IgM (4, 5). Proposing an explanation for the direct relationship, Brambell presented the now widely held hypothesis that IgG is protected from degradation by an Fc receptor–mediated mechanism (6). Specifically, IgG is pinocytosed along with other serum proteins by many cells of the body and is transported to an acidic intracellular compartment where it encounters FcRn, the MHC-related Fc receptor that binds IgG with high affinity at low pH but shows no affinity at physiologic pH (reference 7; for reviews, see references 8 and 9). FcRn effectively diverts IgG from a degradative fate in lysosomes, instead transporting it back to the cell surface where under the influence of neutral pH it dissociates from the receptor and is free to recycle. The lifespan of IgG is thus prolonged relative to other serum proteins not similarly protected. Despite this progress in understanding IgG catabolism, the mechanism by which albumin half-life is prolonged has not been explored.

In 1966, however, Schultze and Heremans conjectured that a mechanism identical to that proposed by Brambell for protecting IgG from degradation could be applied to albumin as well (5). Such a hypothesis has three testable predictions: that FcRn binds albumin in addition to IgG; that FcRn-deficient mice catabolize albumin more rapidly than normal mice; and that the serum albumin concentration in FcRn-deficient mice is low. We have affirmed all three of these predictions.

Materials and Methods

Purification of shFcRn and srFcRn. The Chinese hamster ovary (CHO)* cell line 2G11 secreting recombinant soluble human Fc receptor (shFcRn), given by Dr. Pamela Bjorkman (California Institute of Technology, Pasadena, CA), was cultured in custom

Address correspondence to Dr. Clark Anderson, Department of Internal Medicine, The Ohio State University, 415 HLRI, 473 West 12 Ave., Columbus, OH 43210. Phone: 614-247-7654; Fax: 614-247-7669; E-mail: anderson.48@osu.edu

Abbreviations used in this paper: b2m, β2-microglobulin; CHO, Chinese hamster ovary; HSA, human serum albumin; OG, Octyl-β-D-Glucopyranoside; sRSA, rat serum albumin; shFcRn, soluble human Fc receptor (neonatal).

α MEM Earle's medium (Irvine Scientific) with 5% FCS, penicillin, streptomycin (all from GIBCO BRL), and MSX (Sigma-Aldrich) essentially as described (10). Culture supernatant from these cells containing shFcRn (∼10 mg/liter) in 500 ml batches was acidified to pH 5.8 and applied to a chromatography column containing Sepharose–hIgG (10 ml at substitution ratio of 10 mg hIgG per ml Sepharose) as described (10). Bound shFcRn was eluted at pH 8.1 into 1.0 ml fractions that were assessed for protein content by bicinchoninic acid (BCA) protein assay kit (Pierce Chemical Co.) or UV absorption at 280 nm. shFcRn was further purified by anionic exchange chromatography as described (10). srFcRn was purified from culture supernatant of the CHO cell line 6J23100, also given by Dr. Bjorkman, as described (11).

Quantification of shFcRn-associated BSA. The fractions containing the protein peak of eluted shFcRn were pooled and along with graded amounts of a BSA standard (Pierce Chemical Co.) were analyzed on duplicate SDS-polyacrylamide sizing gels as described (12). One gel was stained with Coomassie blue and the other was processed for immunoblotting with anti-BSA antibody (Sigma-Aldrich) as described (12). The band densities in the Coomassie stained gels were quantified with a Gel Doc system and in immunoblots with a Fluor-S-Max multi-imager using Quantity One software (Bio-Rad Laboratories).

Plasma Protein Concentrations. Albumin and Ig concentrations of mouse plasma samples were determined using sandwich ELISA kits (Bethyl Labs) with reference to standard concentrations of purified proteins as follows: for albumin (Inter-Cell; Cat. no. F301−1) determined by UV absorption at 280 nm using $E^{1\%}_{280} = 5.7$, for IgG isolated from pooled normal mouse serum (Sigma-Aldrich; no. I 5391) determined by UV absorption at 280 nm using $E^{1\%}_{280} = 14.0$, for IgM purified from MOPC 104E ascites (ICN Biomedicals; no. 50335) measured by BCA assay using as a standard BSA quantified by UV absorption at 280 nm, $E^{1\%}_{280} = 6.6$. For IgA the reference serum from the supplier was used as the standard. Plasmas were obtained from The Jackson Laboratory where mice were housed in specific pathogen free barrier facilities. Plasmas were obtained from six mice 8 wk old of a β2-microglobulin (b2m) KO strain (B6.129P2-*B2m^{tm1Unc}*; The Jackson Laboratory; no. 002087) and six mice 8 wk old of their wild-type control strain (C57BL/6J; The Jackson Laboratory; no. 000664); from eight mice of an FcRn α-chain KO strain (B6.129X1/SvJ-*Fcgrt^{Tm1Dcr}*(N6)) (unpublished data) ages 5 wk (n = 3) and 6 wk (n = 3) and 8 wk (n = 2), and 8 mice of their control strain (C57BL/6J, ages 6 wk (n = 3) and 10 wk (n = 5); and from FcRn α-chain KO mice 8 wk old expressing a hFcRn transgene (B6;129-FcRn^{−/−}, hFcRn line 276) and an equal number of transgene negative FcRn KO, littermate controls, 5 in each group. The human FcRn transgene for line 276 was derived from a human FcRn cDNA construct cloned into Vector E (provided by Dr. William Sly, St. Louis University School of Medicine, St. Louis, MO). This transgene is driven by a CMV enhancer and a chicken β-actin promoter, and results in ubiquitous expression as determined by quantitative PCR procedures and Western blot analysis (unpublished data). A similar transgenic has been described (unpublished data).

pH-dependent Binding of shFcRn and srFcRn to Immobilized Ligands. Human serum albumin (HSA; catalog no. A-8763), hIgG (catalog no. I-4506), fish gelatin (catalog no. G-7765), and recombinant sperm whale myoglobin (catalog no. M7526), all from Sigma-Aldrich, and rat serum albumin (RSA; catalog no. 55952) from ICN Biomedicals/Cappel, were immobilized on CNBr-activated Sepharose 4B (Amersham Biosciences) at 10 mg protein/ml Sepharose. Sepharose-Tris was prepared by blocking

the reactive groups of CNBr-activated Sepharose 4B with 0.1 M Trizma base, 0.5 M NaCl, pH 8. Sepharose beads linked to HSA, hIgG, fish gelatin, myoglobin, Tris, or RSA (20 μl beads equivalent to ∼180 μg linked protein) were washed with 50 mM Tris, 150 mM NaCl buffer at pH varying from 5–8 containing 0.1% fish gelatin, and were then incubated for 2 h at room temperature with 80 μl of shFcRn (final concentration 150 μg/ml) in 50 mM Tris, 150 mM NaCl, 0.1% fish gelatin buffer of appropriate pH. Unbound protein was washed away using 50 mM Tris, 150 mM NaCl, 0.1% fish gelatin buffer of appropriate pH. Bound protein was eluted by boiling with SDS-containing sample buffer (60 mM Tris, pH 6.8, 2.3% SDS, 10% glycerol, 0.01% bromophenol blue) containing 1% 2-mercaptoethanol, and was analyzed on a SDS polyacrylamide gel followed by immunoblotting with anti-hFcRn (anti-H1) or anti-rFcRn (1G3; reference 13) antibodies and enhanced chemiluminescence as described (14). The amount of shFcRn or srFcRn bound to the respective immobilized ligands at various pH values was quantified as described above and plotted as a percentage over the amount of protein loaded versus pH. Eluting at pH 8.1, rather than with SDS, and precipitating with trichloroacetic acid (TCA) gave similar results. The amounts of HFE (given by Dr. Pamela Bjorkman) bound to Sepharose-HSA or −myoglobin were analyzed by immunoblotting with anti-b2m antibody (catalog no. sc8362; Santa Cruz Biotechnology, Inc.).

Albumin-shFcRn Interaction in the Presence of Octyl β-D-glucopyranoside. Sepharose-HSA, hIgG, and Tris were prepared as described above for binding at varying pH. Sepharose beads linked to HSA, hIgG, and Tris (20 μl beads equivalent to ∼180 μg linked protein) were washed with 50 mM Tris, 150 mM NaCl, pH 6.0 buffer with 0.1% fish gelatin and varying concentrations of Octyl-β-D-Glucopyranoside (OG; catalog no. O-8001; Sigma-Aldrich), and were then incubated for 2 h at room temperature with 80 μl of shFcRn (final concentration 100 μg/ml) in 50 mM Tris, 150 mM NaCl, 0.1% fish gelatin pH 6.0 buffer of appropriate detergent concentration. Unbound protein was washed away using 50 mM Tris, 150 mM NaCl, 0.1% fish gelatin pH 6.0 buffer of appropriate detergent concentration. Bound protein was eluted, analyzed on a SDS polyacrylamide gel, and quantified as described for the pH experiments. The amount of shFcRn bound to the respective immobilized ligands at various detergent concentrations was plotted as a percentage of total shFcRn versus detergent concentration.

Measurement of Rate of Albumin Decay in FcRn-deficient Mice. All animal studies were approved by the Institutional Review Board. The following murine proteins were used, all purified by a combination of ammonium sulfate precipitation, ionic exchange chromatography, affinity chromatography, and gel filtration; ethanol precipitation was avoided. Albumin (F-301–1, lot 0786) was supplied by Inter-Cell Technologies, Inc. All Ig were obtained from ICN Biomedicals. IgG was an IgG1 myeloma MOPC21 (catalog no. 64335). IgA was myeloma TEPC15 (catalog no. 50326). IgM was myeloma MOPC 104E (catalog no. 50335). These proteins were dialyzed against pH 7.2 buffer containing 50 mM NaCl and 100 mM phosphate, and were radioiodinated by the chlorglycouril method (15) using 5–10 μg CGU per 50–100 μl protein solution. Molar substitution ratios were 0.1–0.2 atoms of ^{125}I per molecule of protein. Two strains of FcRn-deficient mice were used. b2m KO mice (B6.129P2-*B2m^{tm1Unc}*) and its relevant WT control strain (C57BL/6) were obtained from The Jackson Laboratory. FcRn α-chain KO mice were used as well. Development of this strain is described in a separate publication which shows that the FcRn α-chain gene

was disrupted by the targeting vector as predicted; that the mouse expresses no α-chain mRNA or protein; and that it manifests the predicted phenotype, failing to transport IgG across the neonatal gut, degrading IgG at an accelerated rate, and being IgG deficient (unpublished data). Mice at age 3 mo were infused via tail veins with 150 μl radioiodinated protein (2–20 × 10^6 cpm, or 1–12 μg protein) diluted in phosphate buffered saline containing 10% normal mouse serum (ICN Biomedicals). Within 10 min of infusion (time zero) and daily through 120 h, 40 μl blood was sampled via heparinized tubes from the retro-orbital plexus. Plasma was harvested; the proteins in 15 μl plasma were precipitated in 12.5% TCA; radiolabeled proteins in the pellets were counted in a gamma counter and were always >95% of the total radioactivity. The plasma radioactivity, normalized for dose, was plotted on a log scale versus time.

Pharmacokinetic parameter values were determined from the dose-normalized plasma protein concentration-time profiles using WinNonlin software (Pharsight Corp.) and the noncompartmental analysis method. The area under each plasma concentration-time curve (AUC) was calculated using the logarithmic trapezoidal method with the area beyond the last measured value ($C_{p,last}$) estimated from $C_{p,last}/\lambda_z$ where λ_z was the slope of a line fitted by least squares to a plot of the log concentration-time values that appeared to fall along a straight line. Clearance (CL) values for the proteins were calculated from CL = dose/AUC, where dose was cpm infused. Half-life ($t_{1/2}$) was calculated from ln $2/\lambda_z$. The mean $t_{1/2}$ and its standard deviation were calculated using the jack knife technique as described (16).

To calculate the rates of biosynthesis and biodegradation of the proteins, it was assumed that the endogenous proteins were at steady state; i.e., that their rates of biosynthesis equaled their rates of biodegradation. These rates were estimated as the product CL × $C_{p,ss}$, where $C_{p,ss}$ was the steady-state plasma concentration of protein, taken from our measurements.

The radioiodinated protein in plasma at 120 h after infusion of both the FcRn α-chain KO mouse and its WT control mouse was identified as albumin by its mobility on SDS-PAGE (17). Specifically, the 120 h plasma samples were analyzed in parallel with radioiodinated proteins (albumin, IgA, IgM) used for infusion, loading nearly equal cpm in each lane. To deal with the mobility artifact caused by the high concentration of endogenous albumin in plasma, we added unlabeled albumin in the form of normal mouse serum to the infusion protein samples, thereby equalizing the total albumin content of the samples. Radioactive signals in the gel were recorded with a Fluor-S-Multi Imager (Bio-Rad Laboratories).

Calculations. Using the apparent steady-state serum concentrations in mg/ml from Fig. 4 we calculate an albumin/IgG molar plasma ratio of 509 in WT mice in the b2m KO experiments, as follows: ratio = (albumin concentration ÷ albumin gram molecular weight) ÷ (IgG concentration ÷ IgG gram molecular weight) = (31.7 ÷ 67,000) ÷ (0.137 ÷ 150,000) = 509. The biosynthetic rate of albumin, calculated as the product of CL × albumin concentration, in the b2m KO mouse was 0.110 ml/h × 11.5 mg/ml = 1.27 mg/h, and in the WT mouse was 0.072 ml/h × 31.7 mg/ml = 2.28 mg/h. The ratio, then, of WT/KO biosynthetic rates is 2.28 ÷ 1.27 = 1.8.

Comparisons of Ig Concentrations. It would be hazardous to compare the absolute values of our Ig concentrations with those of other laboratories because of differences in age and strain and housing conditions of the mice and because of differences in assay reagents. Likewise, within our own data of Fig. 5 one should only cautiously compare between Ig classes because the assays for

each class may vary in efficiency, each requiring its own standard and its own anti-Ig antibody. Nevertheless, it would appear that our IgG values (113–139 μg/ml) are not disparate from what has been reported. IgG levels are well known to be very low in mice reared in relative germ-free conditions similar to ours housed in specific pathogen free facilities. Specifically, IgG concentrations in 8-wk-old C57BL/6 mice were reported to be 33 μg/ml (18), while Balb/c mice gave values ranging from 3 μg/ml (19) to 56 μg/ml (20). Values as high as 20 mg/ml have been reported for mice raised conventionally (21). Similarly, while our reported IgA concentrations might seem high (237–482 μg/ml), others have reported concentrations far in excess of ours, e.g., 0.6–2.3 mg/ml (22) and 1–3 mg/ml (21). Thus, we argue that comparisons should legitimately be made only for each antibody between the two strains of mice (KO and WT). Likewise, comparisons between albumin and IgG concentrations should be considered approximate.

Results

First, we found fortuitously that albumin binds FcRn to form a tri-molecular complex with IgG. Upon eluting recombinant soluble human FcRn (shFcRn) from an IgG affinity matrix by raising the pH from 5.8 to 8.1 we noted a 67-kD protein copurifying in abundance with shFcRn. In a typical experiment, acidified culture supernatant of a transfected cell line (CHO) secreting shFcRn (10), a heterodimer of the extracellular portion of the α-chain and β2-microglobulin (b2m), was passed through an affinity column of Sepharose-human IgG (hIgG). The protein peak in several fractions of the pH 8.1 eluate was analyzed by electrophoresis on a sizing gel (Fig. 1 A). Three prominent bands were apparent: the 35-kD truncated shFcRn α-chain identified in other experiments by immunoblotting; a 12-kD b2m run off the gel shown, identified also by immunoblotting in other experiments; and a 67-kD band. Elution of the 67-kD molecule was dependent on the presence of shFcRn; i.e., it was not affinity purified in like manner from culture supernatant of CHO cells not secreting shFcRn. It was apparent in Fig. 1 A and in many such experiments that while the elution profiles of shFcRn and the 67-kD protein overlapped, the 67-kD protein peak eluted at a slightly more acidic pH (fraction 6) than did shFcRn (between fraction 6 and 7). This consistent lag suggested that the 67-kD protein interacted with shFcRn in a pH dependent fashion, just as did IgG. The 67-kD molecule was not simply eluting bound to shFcRn; rather, the tri-molecular complex was dissociating into its three components at basic pH.

The 67-kD protein (lane E of Fig. 1 B, top) had the mobility of BSA by reference to BSA standards in adjacent lanes and was identified as BSA by immunoblotting (Fig. 1 B, bottom). Further, densitometric quantification of both the Coomassie stained image (Fig. 1 B, top) and the immunoblotted image (Fig. 1 B, bottom) gave virtually identical values (Fig. 1 C), suggesting that this band was entirely BSA. In a series of experiments the molar ratio of shFcRn to BSA in eluates has varied from close to unity to ~10 for reasons that so far elude us. The obvious source of BSA was the 10% FCS
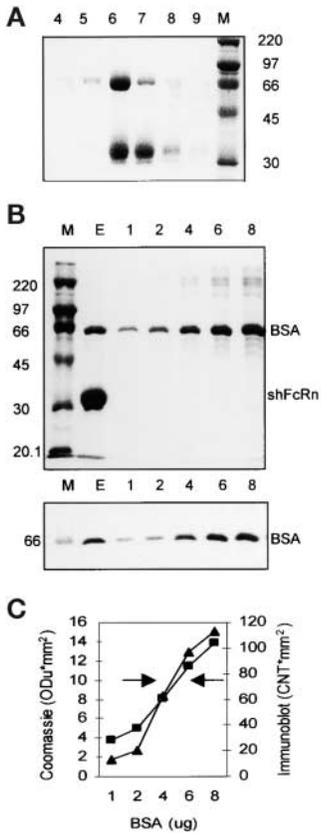
Figure 1. Copurification of BSA and shFcRn by affinity chromatography on Sepharose-hIgG. (A) Culture supernatant from CHO cells secreting recombinant shFcRn was acidified to pH 5.8 and applied to a Sepharose-hIgG chromatography column. Bound shFcRn was eluted at pH 8.1. Six fractions of the elution peak (4–9) were analyzed by SDS-PAGE under reducing conditions and Coomassie blue staining. The molecular weight markers (M, in kD) allow identification of the α-chain of shFcRn at ∼35kD and another copurifying protein at 67kD. (B) The elution peak (E) from a Sepharose IgG column was analyzed by SDS-PAGE on two identical gels along with molecular weight standards (M) and graded amounts (lanes 1–8; in μg per lane) of BSA. One gel (top) was stained with Coomassie blue and the other (bottom) was immunoblotted with anti-BSA antibody. (C) The band densities in the Coomassie stained gel (■) and the immunoblot (▲) of B were plotted (on y-axis) against BSA quantity (on x-axis). The left arrow indicates the eluate density on the Coomassie stained gel while the right arrow indicates the density of the eluate on the immunoblot. Three separate experiments have given equivalent results.

present in the growth medium of the CHO cells. It is important to note that no proteins other than BSA were copurified with shFcRn from FCS despite many being present in concentrations far in excess of the ∼10 μg/ml of shFcRn.

Using a different approach, we assessed more rigorously the acid dependence of albumin–shFcRn interaction by comparing the capacity of shFcRn to bind to both Sepharose-human serum albumin (HSA) and Sepharose-hIgG in buffers ranging from pH 5.0–8.0. After binding to immobilized ligands, shFcRn was eluted and the eluted protein was quantified by densitometry of anti-FcRn immunoblots (Fig. 2, A–D). Binding of shFcRn to both Sepharose-HSA (Fig. 2 A) and Sepharose-hIgG (Fig. 2 B) was pH dependent, being maximal at pH 5.0 with ∼80% of total receptor being adsorbed from solution; binding was nil at pH 7.0 through pH 8. At intermediary pH values the binding of shFcRn was slightly greater to HSA at lower pH and slightly greater to hIgG at higher pH, noted both in Fig. 2 D and in two other similar experiments not shown; the differences are subtle, however, and will require further study. Binding to Sepharose-Tris (Fig. 2 C) and to both Sepharose-fish gelatin and Sepharose-myoglobin (unpublished data) was nil throughout the pH range. In similar experiments we have found that shFcRn binds to immobilized albumin from rat, mouse, and bovine (unpublished data).
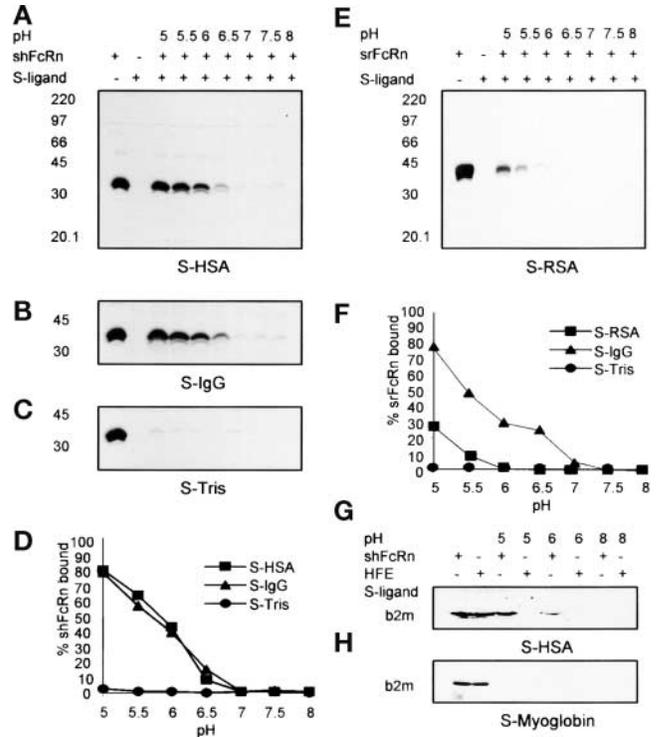

Figure 2. pH-dependent binding of FcRn to immobilized albumin. Sepharose (S)-HSA, S-IgG, S-Tris, S-fish gelatin (see Materials and Methods), or S-RSA were incubated with shFcRn or srFcRn at varying pH as shown. Bound soluble FcRn were eluted and were quantified by immunoblotting with anti-FcRn antibody. Immunoblots of binding of shFcRn to S-HSA, S-IgG, and S-Tris at pH values indicated are shown in A, B, and C, respectively. Immunoblot of binding of srFcRn to S-RSA is shown in E. The positions of molecular weight markers (M, in kD) are shown. Lane 1 in all the gels contained 15 μg soluble FcRn, the amount added to every adsorbent sample. Lane 2 in each case shows the eluate from Sepharose-ligand in the absence of FcRn. The shFcRn bands were quantified and are plotted in panel D vs. pH. Three distinct experiments have given equivalent results. srFcRn band densities are plotted in panel F vs. pH. A second experiment with srFcRn gave equivalent results. G and H show binding of HFE to S-HSA and S-myoglobin. Lanes 1 and 2 show amounts of shFcRn and HFE added (15 μg) to adsorbent samples. Bound protein was eluted and quantified by blotting with anti-b2m antibody.

Assessing FcRn from another species, the rat, we noted that soluble rat FcRn (srFcRn) bound Sepharose-linked rat albumin (Fig. 2 E) at acidic pH although to a lesser extent than to Sepharose-hIgG (Fig. 2 F). srFcRn did not, however, bind Sepharose-human and -bovine albumin, nor did it bind Sepharose-Tris or -myoglobin (unpublished data). Assessing another nonclassical MHC1 family member, namely, HFE (23), implicated in hereditary hemochromatosis, we found no binding of HFE to Sepharose-HSA while shFcRn simultaneously bound (Fig. 2 G). Neither HFE nor shFcRn bound Sepharose-myoglobin (Fig. 2 H).

It would be predicted that we should be able to purify native (as opposed to recombinant) FcRn on immobilized albumin at the appropriate pH. However, our attempts to affinity adsorb native FcRn from detergent lysates of FcRn expressing tissue such as placenta, skin, and an FcRn-expressing cell line (MRC5) have so far failed, al-
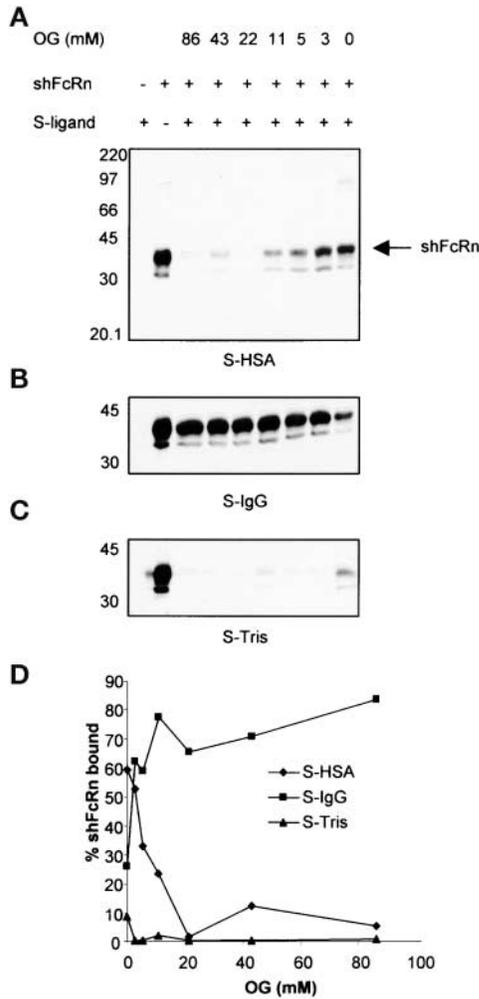
Figure 3. Detergent inhibits shFcRn albumin interaction. Sepharose (S)-HSA, S-IgG and S-Tris (A–C) were incubated with shFcRn in a pH 6.0 buffer containing indicated concentrations of OG as shown. Bound shFcRn was eluted and quantified by immunoblotting with anti-FcRn antibody. The positions of molecular weight markers (M, in kD) are shown. Lane 1 in each case shows the eluate from Sepharose-ligand in the absence of shFcRn. Lane 2 in all the gels contained 10 μg shFcRn, the amount added to every adsorbent sample. The shFcRn bands were quantified and plotted in panel D vs. OG concentration. Similar results were obtained in another experiment.

though the native receptor is readily adsorbed by immobilized IgG (14, 24, 25). Offering a potential explanation for this observation, we found that nonionic detergent (either OG or TX100) completely inhibits capture of recombinant shFcRn with immobilized albumin. As Fig. 3 shows, complete blockade (97%) was achieved with as little as 22 mM OG (essentially, the critical micellar concentration), far less than the concentration used for tissue or cell dissolution (86 mM). In contrast, the capture of shFcRn with immobilized IgG was preserved and in fact was enhanced in OG (2.5-fold at 22 mM and 3.2-fold at 86 mM). Whether detergent interferes with the albumin binding site or the receptor binding site, or both, we have not yet been able to ascertain.
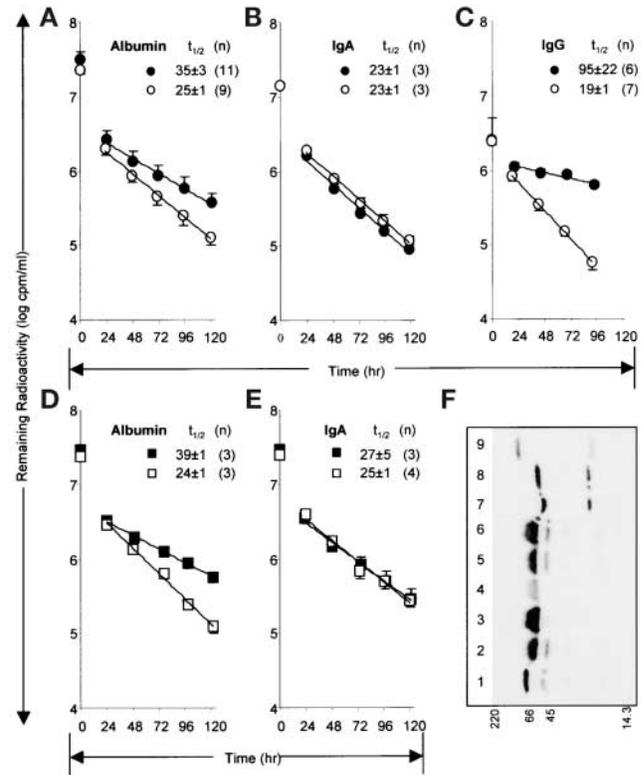

Figure 4. Decay of radioiodinated albumin in FcRn-deficient mice. A–C show the concentration of plasma radioactivity remaining at indicated times after intravenous infusion of b2m KO mice (open circles) and their WT control mice (filled circles) of radioiodinated albumin, IgA, and IgG, respectively. D and E show results for FcRn α-chain KO (open squares) and WT control mice (filled squares). Mean half-lives ($t_{1/2}$) of β-phase decay in hours are shown with SD. The numbers of mice in each experiment are indicated by (n). Using a repeated measures ANOVA model to compare results between b2m KO and WT animals, we analyzed the logarithm of the ratio of the daily values with time 0 values (log ratios of plasma cpm). We found a statistically significant difference between the two groups of animals in the half-lives of both albumin and IgG during days 1 to 5 (both P values <0.0001). IgA and IgM (text only) values in the two strains of mice were not significantly different from one another (P = 0.4 and 0.9, respectively). For the experiment with FcRn α-chain KO and WT, the P value for albumin was <0.0001 while that for IgA was 0.3. F shows an autoradiograph of an SDS-PAGE of the radiolabeled proteins in the plasma of WT (lane 3) and FcRn α-chain KO (lane 4) mice at 120 h after infusion of radiolabeled albumin. The positions of molecular weight markers (M, in kD) are shown along bottom. Lanes 1, 2, 5, and 6 contain infused radiolabeled albumin equalized for the endogenous albumin content of the plasma samples by the addition, respectively, of 0, 0.75, 0.5, and 1.5 μl normal mouse plasma. Lanes 7 and 8 contain radioiodinated IgA containing 0 and 1.5 μl mouse serum, respectively. Lane 9 contains radioiodinated IgM. The experiment was repeated with 120 h plasma from a b2m KO mouse and WT control with equivalent results.

Testing the second prediction of the Schultze/Heremans hypothesis, that albumin will be degraded more rapidly in mice deficient in FcRn, we infused radioiodinated mouse albumin intravenously into mice of two strains deficient in FcRn, both the b2m KO strain (26) and the FcRn α-chain KO strain (unpublished data). By sampling blood daily for 120 h we calculated the albumin decay curves (plotted in Fig. 4, A–E) and the half-lives from the β- or elimination-phase
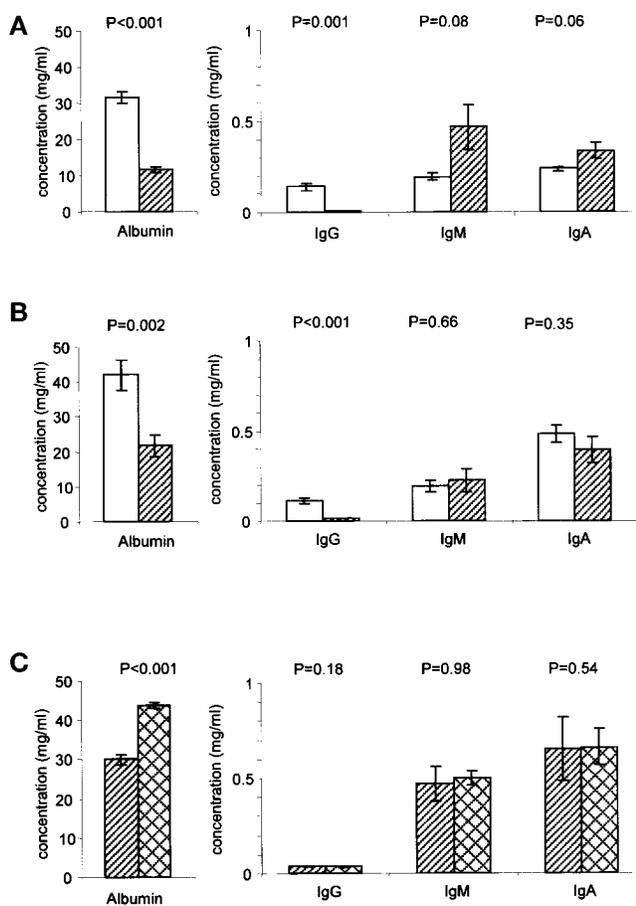
Figure 5. Plasma concentrations of albumin, IgG, IgA, and IgM in FcRn-deficient mice and in FcRn α–chain–deficient mice expressing a hFcRn transgene. Concentrations were determined by a sandwich ELISA. The specific KO, WT, transgenic strains and ages are given in Materials and Methods. Values are the means ± standard errors. P values are from Student's *t* test. Alternative significance statements using the nonparametric Mann-Whitney test give comparable results. (A) b2m KO (hatched bars) and corresponding wild-type (empty bars), six mice in each group. (B) FcRn α–chain KO (hatched bars) and corresponding wild-type (empty bars), eight mice in each group. (C) FcRn α–chain KO mice either expressing (crosshatched bars) or not expressing (hatched bars) a hFcRn transgene, five mice in each group.

of decay (having no data for the first 24 h save for the zero point, we ignore the α- or distribution-phase calculations, although in a single pilot experiment with 3 mice we note $t_{1/2}$ of the α-phase to be <4 h.) It can be seen that the half-life of albumin is shortened in the b2m KO strain ($t_{1/2}$ 25 h vs. 35 h in WT, Fig. 4 A) whereas the half-lives of IgA are not different in the two strains ($t_{1/2}$ 23 h, Fig. 4 B). IgM decay curves were superimposable on those of Fig. 4 B ($t_{1/2}$ 23 ± 1 in both strains of mice). As well, the half-life of IgG is shortened ($t_{1/2}$ 19 h vs. 95 h in WT, Fig. 3 C), as has already been reported (22, 27, 28). Others have noted but not explored a modest increase in the decay rate of albumin in b2m KO mice (27, 29). As b2m KO mice are not albuminuric (30, 31), we suggest the rapid decay represents degradation.

Likewise, in the FcRn α–chain KO strain (Fig. 4, D and E), albumin half-life is shortened ($t_{1/2}$ 24 h vs. 39 h in WT, Fig. 4 D) while that of IgA is not (Fig. 4 E); and, although

not shown here, IgG half-life is shortened (unpublished data). Because the amount of radioiodinated protein remaining at the end of the 120 h experiment was a small fraction of that infused at time zero, we considered experimentally whether the remaining labeled protein was indeed albumin. Analyzing the 120 h plasma samples from FcRn α–chain KO and WT mice by SDS-sizing gel electrophoresis and PhosphorImaging, we noted (Fig. 4 F) that the radioactive bands from both KO and WT mice (lanes 3 and 4) were indistinguishable in mobility from the ^{125}I-albumin infusion samples adjusted for the high endogenous albumin content of the plasma samples by the addition of exogenous normal mouse plasma (lanes 2, 5, 6). This observation largely eliminates the possibility that decay of a small contaminant of the albumin preparation was responsible for the differences noted in decay rates.

It would be predicted by the Schultze/Heremans hypothesis that a lower serum albumin concentration and/or an increased albumin biosynthetic rate in FcRn-deficient mice would accompany an accelerated rate of degradation. Measuring the former we found that in both FcRn-deficient strains tested the serum albumin concentrations were ~45% of that in control strains (Figs. 5 A and 4 B). IgA and IgM concentrations were not diminished in b2m KO mice compared with WT mice (Fig. 5 A), and in fact were marginally significantly higher. IgA and IgM concentrations were not different statistically between the FcRn α–chain KO and WT strains (Fig. 5 B). As has been shown before, IgG concentrations were low in the FcRn-deficient strains compared with WT strains (22, 27; unpublished data).

The relative albumin deficiency in the FcRn α–chain KO mouse was corrected (increased by 46%) by the expression of an hFcRn transgene (Fig. 5 C), while IgG, IgM, and IgA concentrations were not affected. This result eliminates the possibility that genes flanking the FcRn targeting vector in the original host embryonic stem cell are responsible for the noted rapid decay of albumin in the FcRn α–chain KO mouse. Moreover, this result suggests that the human FcRn binds and protects murine albumin from degradation. We have incidentally found, as corroborated by the IgG data of Fig. 5 C, that the human transgenic receptor is not as promiscuous in its handling of IgG of different species as it is in its handling of albumin of different species; i.e., it is unable to bind and protect murine IgG from degradation although its presence corrects the rapid decay rate of infused human IgG in the FcRn α–chain KO mouse (unpublished data).

Discussion

These three independent results, we conclude, affirm the hypothesis that FcRn binds not only IgG but albumin as well, salvaging both proteins from a degradative fate and extending their lifespans.

Our observation that FcRn binds albumin in the same pH dependent fashion as it binds IgG suggests that the mechanism of protection of albumin by FcRn is identical to that of IgG, as postulated by Shultze and Heremans. We

envision that albumin is pinocytosed nonspecifically along with IgG from the extracellular milieu, is transported to acidic endosomes where it binds FcRn, is thereby diverted from the lysosomal degradation pathway, is exocytosed intact, and is then free to transit again, thus extending its half-life. That this albumin protection mechanism is widespread among animals is suggested by our data from three species, i.e., binding data using both human and rat FcRn, and albumin decay rates and plasma concentrations in the mouse. Further, the fact that the $t_{1/2}$ of albumin in both KO strains compared with WT were approximately equal would suggest that FcRn accounts for the entire protection effect conferred by b2m-associated proteins; i.e., no other MHC related molecule need be implicated in the protection from decay of albumin. The failure of HFE to bind albumin (Fig. 2 G) supports this conclusion.

Using the kinetic data of Fig. 4 and the apparent steady state protein concentrations recorded in Fig. 5 we can compare the relative capacity of FcRn to protect albumin and IgG from degradation. From the dose administered and the rate of elimination we compute albumin clearance for the b2m KO strain and its relevant WT control strain to be 0.110 and 0.072 ml/h, respectively; while for IgG the respective clearances for the two strains are 0.043 and 0.015 ml/h. We reason that the fraction of protein saved per day by FcRn would be directly related to the difference between the clearances in WT and KO strains; namely, 0.038 ml/h for albumin and 0.028 ml/h for IgG. Based on a molar ratio of serum albumin to IgG of 509 from Fig. 4 A, we calculate (see Materials and Methods) that for every molecule of IgG saved from degradation by FcRn, almost 700 molecules of albumin are saved from degradation! Thus, what would appear to be a minor difference in the rate of albumin decay between WT and KO is magnified by the widely disparate serum concentrations of the two proteins to reveal an extraordinary capacity of FcRn to handle albumin relative to IgG. The low IgG concentrations in these mice are likely the result of pathogen free housing (see note on comparisons of Ig concentrations in Materials and Methods). Yet, were we to extrapolate to the human, where the concentrations of these two proteins are not so disparate (IgG and albumin, 10 and 40 mg/ml, respectively), the molar ratio of albumin to IgG saved by FcRn would be 12, still many more albumin than IgG molecules.

We can further apply the kinetic data of Fig. 4 to a calculation of the albumin biosynthetic rate in FcRn-deficient mice where biosynthetic rate (mg/h) = clearance (ml/h) × steady state plasma concentration (mg/ml) from our steady state data. We find for the b2m KO strain and its relevant WT control that the biosynthetic rate in the WT is 1.8-fold greater than that of the KO (2.28 mg/h vs. 1.27 mg/h). This result implicates FcRn in the albumin biosynthetic pathway.

The question emerges whether FcRn transports albumin as it does IgG from mother to offspring. Brambell in his 1970 monograph summarizing this entire area at that time asserted that in most if not all animals albumin was transmitted along with IgG although to a lesser extent (6). The published data,

however, are old, scant, sketchy, and conflicting; and it would appear that interest in examining albumin transport was very early eclipsed by the more compelling question of IgG transport. This issue will require revisiting.

Whether FcRn plays a role in the transit of albumin between the vascular and the extravascular spaces is an enticing question. In support of this notion, endothelium has not only been suggested as the likely main site of albumin degradation (32), implying abundant uptake, but it also has been shown to be a site of FcRn expression (22, 33; unpublished data). One prediction of such a hypothesis is that the rate of distribution to the extravascular space after an albumin infusion may be slowed in FcRn-deficient mice.

We note that albumin is found in the lamprey and so predates immunoglobulin in evolutionary history (1, 34). Moreover, elements of the albumin family appear as ancient as Phylum Echinodermata (35). Thus, we would suggest the existence of an FcRn precursor that bound only albumin as the evolutionary antecedent to the present day FcRn that binds both albumin and IgG. It seems not too far-fetched to conjecture that such an antecedent may have evolved as well into an MHC-like peptide-binding molecule.

References

1. Peters, T., Jr. 1996. All About Albumin: Biochemistry, Genetics, and Medical Applications. Academic Press, New York.
2. Freeman, T., and A.H. Gordon. 1965. Albumin catabolism in hypoproteinaemic states studied with ^{131}I-Albumin. *Bibl. Haematol.* 1108–1115.
3. Cormode, E.J., D.M. Lyster, and S. Israels. 1975. Analbuminemia in a neonate. *J. Pediatr.* 86:862–867.
4. Waldmann, T.A., and W. Strober. 1969. Metabolism of immunoglobulins. *Prog. Allergy.* 13:1–110.
5. Schultze, H.E., and J.F. Heremans. 1966. Molecular biology of human proteins: with special reference to plasma proteins. Vol. 1. *In* Nature and Metabolism of Extracellular Proteins. Elsevier, New York. 904 pp.
6. Brambell, F.W.R. 1970. The Transmission of Passive Immunity from Mother to Young. North Holland Publishing Company, Amsterdam. 385 pp.
7. Simister, N.E., and K.E. Mostov. 1989. An Fc receptor structurally related to MHC class I antigens. *Nature.* 337:184–187.
8. Junghans, R.P. 1997. The Brambell receptor (FcRB): mediator of transmission of immunity and protection from catabolism for IgG. *Immunol. Res.* 16:29–57.

9. Ghetie, V., and E.S. Ward. 2000. Multiple roles for the major histocompatibility complex Class I-related receptor FcRn. *Annu. Rev. Immunol.* 18:739–766.

10. West, A.P., Jr., and P.J. Bjorkman. 2000. Crystal structure and immunoglobulin G binding properties of the human major histocompatibility complex-related Fc receptor. *Biochemistry.* 39:9698–9708.

11. Gastinel, L.N., N.E. Simister, and P.J. Bjorkman. 1992. Expression and crystallization of a soluble and functional form of an Fc receptor related to class I histocompatibility molecules. *Proc. Natl. Acad. Sci. USA.* 89:638–642.

12. Tridandapani, S., K. Siefker, J.-L. Teillaud, J.O. Carter, M.D. Wewers, and C.L. Anderson. 2002. Regulated expression and inhibitory function of FcγRIIb in human monocytic cells. *J. Biol. Chem.* 277:5082–5089.

13. Raghavan, M., M.Y. Chen, L.N. Gastinel, and P.J. Bjorkman. 1994. Investigation of the interaction between the class I MHC-related Fc receptor and its immunoglobulin G ligand. *Immunity.* 1:303–315.

14. Leach, J.L., D.D. Sedmak, J.M. Osborne, B. Rahill, M.D. Lairmore, and C.L. Anderson. 1996. Isolation from human placenta of the IgG transporter, FcRn, and localization to the syncytiotrophoblast: Implications for maternal-fetal antibody transport. *J. Immunol.* 157:3317–3322.

15. Fraker, P.J., and J.C. Speck, Jr. 1978. Protein and cell membrane iodinations with a sparingly soluble chloroamide, 1,3,4,6,-tetrachloro-3a,6a-diphenylglycoluril. *Biochem. Biophys. Res. Comm.* 80:849–857.

16. Lam, F.C., C.T. Hung, and D.G. Perrier. 1985. Estimation of variance for harmonic mean half-lives. *J. Pharm. Sci.* 74:229–231.

17. Laemmli, U.K. 1970. Cleavage of structural proteins during the assembly of the head of bacteriophage T4. *Nature.* 227:680–685.

18. Senda, S., E. Cheng, and H. Kawanishi. 1989. IgG in murine intestinal secretions: Aging effect and possible physiological role. *Scand. J. Immunol.* 29:41–47.

19. Natsuume-Sakai, S., K. Motonishi, and S. Migita. 1977. Quantitative estimations of five classes of immunoglobulin in inbred mouse strains. *Immunology.* 32:861–866.

20. Bos, N.A., H. Kimura, C.G. Meeuwsen, H.D. Visser, M.P. Hazenberg, B.S. Wostmann, J.R. Pleasants, R. Benner, and D.M. Marcus. 1989. Serum immunoglobulin levels and naturally occurring antibodies against carbohydrate antigens in germ-free BALB/c mice fed chemically defined ultrafiltered diet. *Eur. J. Immunol.* 19:2335–2339.

21. Goding, J.W. 1986. Monoclonal Antibodies: Principles and Practice. Harcourt Brace Jovanovich, London. 114 pp.

22. Ghetie, V., J.G. Hubbard, J.-K. Kim, M.-F. Tsen, Y. Lee, and E.S. Ward. 1996. Abnormally short serum half-lives of IgG in β2-microglobulin-deficient mice. *Eur. J. Immunol.* 26:690–696.

23. Feder, J.N., A. Gnirke, W. Thomas, Z. Tsuchihashi, D.A. Ruddy, A. Basava, F. Dormishian, R. Domingo, Jr., M.D. Ellis, A. Fullan, et al. 1996. A novel MHC class I-like gene is mutated in patients with hereditary haemochromatosis. *Nat. Genet.* 13:399–408.

24. Roberts, D.M., M. Guenthert, and R. Rodewald. 1990. Isolation and characterization of the Fc receptor from the fetal yolk sac of the rat. *J. Cell Biol.* 111:1867–1876.

25. Zhu, X., G. Meng, B.L. Dickinson, X.T. Li, E. Mizoguchi, L.L. Miao, Y.S. Wang, C. Robert, B.Y. Wu, P.D. Smith, et al. 2001. MHC Class I-related neonatal Fc receptor for IgG is functionally expressed in monocytes, intestinal macrophages, and dendritic cells. *J. Immunol.* 166:3266–3276.

26. Koller, B.H., P. Marrack, O. Kappler, and O. Smithies. 1990. Normal development of mice deficient in B2M, MHC, and CD8+ T cells. *Science.* 248:1227–1230.

27. Junghans, R.P., and C.L. Anderson. 1996. The protection receptor for IgG catabolism is the β2-microglobulin-containing neonatal intestinal transport receptor. *Proc. Natl. Acad. Sci. USA.* 93:5512–5516.

28. Israel, E.J., D.F. Wilsker, K.C. Hayes, D. Schoenfeld, and N.E. Simister. 1996. Increased clearance of IgG in mice that lack B2-microglobulin: possible protective role of FcRn. *Immunology.* 89:573–578.

29. Telleman, P., and R.P. Junghans. 2000. The role of the Brambell receptor (FcRB) in liver: protection of endocytosed immunoglobulin G (IgG) from catabolism in hepatocytes rather than transport of IgG to bile. *Immunology.* 100:245–251.

30. Mozes, E., L.D. Kohn, F. Hakim, and D.S. Singer. 1993. Resistance of MHC class I-deficient mice to experimental systemic lupus erythematosus. *Science.* 261:91–93.

31. Mixter, P.F., J.Q. Russell, F.H. Durie, and R.C. Budd. 1995. Decreased CD4-CD8- TCR-alpha beta + cells in lpr/lpr mice lacking beta 2-microglobulin. *J. Immunol.* 154:2063–2074.

32. McFarlane, A.S. 1957. The behavior of I^{131}-labeled plasma proteins *in vivo. Ann. NY Acad. Sci.* 70:19–25.

33. Borvak, J., J. Richardson, C. Medesan, F. Antohe, C. Radu, M. Simionescu, V. Ghetie, and E.S. Ward. 1998. Functional expression of the MHC class I-related receptor, FcRn, in endothelial cells of mice. *Int. Immunol.* 10:1289–1298.

34. Flajnik, M.F., and M. Kasahara. 2001. Comparative genomics of the MHC: glimpses into the evolution of the adaptive immune system. *Immunity.* 15:351–362.

35. Soltysik-Española, M., D.C. Klinzing, K. Pfarr, R.D. Burke, and S.G. Ernst. 1994. Endo 16, a large multidomain protein found on the surface and ECM of endodermal cells during sea urchin gastrulation, binds calcium. *Dev. Biol.* 165:73–85.